

## Article

# Nitrogen-Containing Secondary Metabolites from a Deep-Sea Fungus *Aspergillus unguis* and Their Anti-Inflammatory Activity

Cao Van Anh <sup>1,2</sup>, Yeo Dae Yoon <sup>3</sup>, Jong Soon Kang <sup>3</sup>, Hwa-Sun Lee <sup>1</sup> , Chang-Su Heo <sup>1,2</sup> and Hee Jae Shin <sup>1,2,\*</sup> 

<sup>1</sup> Marine Natural Products Chemistry Laboratory, Korea Institute of Ocean Science and Technology, 385 Haeyang-ro, Yeongdo-gu, Busan 49111, Korea; caovananh@kiost.ac.kr (C.V.A.); hwasunlee@kiost.ac.kr (H.-S.L.); science30@kiost.ac.kr (C.-S.H.)

<sup>2</sup> Department of Marine Biotechnology, University of Science and Technology (UST), 217 Gajungro, Yuseong-gu, Daejeon 34113, Korea

<sup>3</sup> Laboratory Animal Resource Center, Korea Research Institute of Bioscience and Biotechnology, 30 Yeongudanjiro, Cheongju 28116, Korea; yunyd76@kribb.re.kr (Y.D.Y.); kanjon@kribb.re.kr (J.S.K.)

\* Correspondence: shinhj@kiost.ac.kr; Tel.: +82-51-664-3341; Fax: +82-51-664-3340

**Abstract:** *Aspergillus* is well-known as the second-largest contributor of fungal natural products. Based on NMR guided isolation, three nitrogen-containing secondary metabolites, including two new compounds, variotin B (1) and coniosulfide E (2), together with a known compound, unguisin A (3), were isolated from the ethyl acetate (EtOAc) extract of the deep-sea fungus *Aspergillus unguis* IV17-109. The planar structures of 1 and 2 were elucidated by an extensive analysis of their spectroscopic data (HRESIMS, 1D and 2D NMR). The absolute configuration of 2 was determined by comparison of its optical rotation value with those of the synthesized analogs. Compound 2 is a rare, naturally occurring substance with an unusual cysteinol moiety. Furthermore, 1 showed moderate anti-inflammatory activity with an IC<sub>50</sub> value of 20.0 μM. These results revealed that *Aspergillus unguis* could produce structurally diverse nitrogenous secondary metabolites, which can be used for further studies to find anti-inflammatory leads.

**Keywords:** deep-sea fungus; *A. unguis*; variotin; coniosulfide; anti-inflammatory



**Citation:** Anh, C.V.; Yoon, Y.D.; Kang, J.S.; Lee, H.-S.; Heo, C.-S.; Shin, H.J.

Nitrogen-Containing Secondary Metabolites from a Deep-Sea Fungus

*Aspergillus unguis* and Their

Anti-Inflammatory Activity. *Mar.*

*Drugs* **2022**, *20*, 217. <https://doi.org/10.3390/md20030217>

10.3390/md20030217

Academic Editors:

Donatella Degl'Innocenti and

Marzia Vasarri

Received: 2 March 2022

Accepted: 19 March 2022

Published: 20 March 2022

**Publisher's Note:** MDPI stays neutral with regard to jurisdictional claims in published maps and institutional affiliations.



**Copyright:** © 2022 by the authors. Licensee MDPI, Basel, Switzerland. This article is an open access article distributed under the terms and conditions of the Creative Commons Attribution (CC BY) license (<https://creativecommons.org/licenses/by/4.0/>).

## 1. Introduction

Deep-sea hydrothermal vents are recognized as one of the most extreme and dynamic habitats on our planet [1]. These hotspot ecosystems are characterized by high temperature, high pressure, low oxygen supply, and the absence of sun light [2]. In addition, hydrothermal vent flows bring fluids with high concentrations of reduced sulfur-containing compounds and heavy metals [2]. Given this fact, microorganisms living in this specific environment are considered as a new frontier for discovery of natural products with unique structures and tremendous pharmacological activities [3].

*Aspergillus* is renowned as a prolific source of numerous fungal peptides, including lipo-, depsi-, linear-, and cyclic-peptides, which are structurally unique and demonstrated various bioactivities, such as anti-microbial, anti-fungal, anti-inflammatory, and cytotoxic activities [4,5]. Among the peptides derived from *Aspergillus* spp., unguisins are a unique cyclic heptapeptide class commonly produced by *Aspergillus unguis*, and until now unguisins A–G have been reported [6,7].

Inflammation is a protective response of our body to a wide range of stimuli. This process plays a central role or is an important symptom in the pathogenesis of various chronic diseases for instance Alzheimer's disease, asthma, diabetes, and rheumatoid arthritis [8]. The inflammatory process is characterized by over secretion of nitric oxide (NO) and inflammatory cytokines such as interleukin 1 beta (IL-1β), tumor necrosis factor alpha (TNF-α), and interleukin 6 (IL-6). Therefore, reducing the production of inflammatory mediators is a key indicator for the treatment of various diseases.

As part of our study on marine-derived microorganisms isolated near hydrothermal vents, we have reported some anti-inflammatory phenazine alkaloids from a yeast-like fungus *Cystobasidium laryngis*, and nidulin-related polyketides from *A. unguis* IV17-109, which showed anti-microbial and cytotoxic activities [9,10]. Based on NMR guided isolation, we found that the  $^1\text{H}$  NMR spectra of non-polar fractions from *A. unguis* IV17-109 showed some minor interesting peaks in the olefinic region, which do not belong to unguisin peptides or nidulin-related polyketides. Further careful purification of these fractions led to the identification of two new compounds, variotin B (**1**) and coniosulfide E (**2**) (Figure 1). Anti-inflammatory activity of **1** and **2** was preliminarily evaluated and the result revealed that **1** has moderate activity. Here, we report the details of the isolation, structure identification, and anti-inflammatory nature of these compounds.

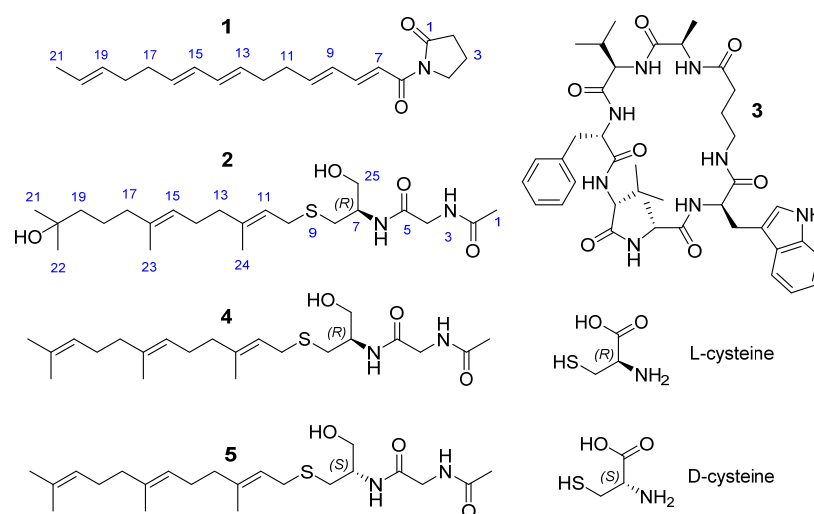


**Figure 1.** Structures of **1–3** isolated from *A. unguis* IV17-109, and the synthetic analogs (**4** and **5**).

## 2. Results and Discussion

Compound **1** was isolated as pale-yellow needles with the molecular formula of  $\text{C}_{20}\text{H}_{27}\text{NO}_2$  based on its HRESIMS peak at  $m/z$  336.1938,  $([\text{M}+\text{Na}]^+)$ , calculated for  $\text{C}_{20}\text{H}_{27}\text{NO}_2\text{Na}$ , 336.1939), requiring 8 indices of hydrogen deficiency. The  $^1\text{H}$  NMR spectrum of **1** showed signals attributed to a methyl group at  $\delta_{\text{H}}$  1.62 (d,  $J = 4.5$ ,  $\text{H}_3$ -21), seven methylene groups at  $\delta_{\text{H}}$  2.04–3.82, and ten olefinic protons at  $\delta_{\text{H}}$  5.42–7.37. The  $^{13}\text{C}$  NMR spectrum in combination with HSQC data revealed signals of 20 resonances belonging to a methyl at  $\delta_{\text{C}}$  18.1, seven methylene carbons at  $\delta_{\text{C}}$  18.1–47.0, ten olefinic carbons at  $\delta_{\text{C}}$  121.7–146.9, and two carbonyl carbons at  $\delta_{\text{C}}$  168.2 and 177.8. Two carbonyl and ten  $\text{sp}^2$  carbons, accounting for 7 out of 8 degrees of unsaturation, indicated **1** is a monocyclic compound. The structure of a five-membered lactam ring was determined by continuous  $^1\text{H}$ - $^1\text{H}$  COSY correlations from  $\text{H}_2$ -2 to  $\text{H}_2$ -4, and the HMBC correlation from  $\text{H}_2$ -4 to C-1. A substructure was identified as a C-16 polyunsaturated fatty acid by continuous  $^1\text{H}$ - $^1\text{H}$  COSY correlations from H-7 to  $\text{H}_3$ -21, and the HMBC correlations from H-7 and H-8 to C-6 (Figure 2). The connection of the fatty acid and the lactam ring was corroborated by the HMBC correlation from  $\text{H}_2$ -4 to C-6.

The geometries of  $\Delta^{7,9,13,15}$  were deduced as *E*-form by their large coupling constants (Table 1) and the chemical shift of terminal methyl (C-21) was  $\delta_{\text{C}}$  18.1, revealing the geometry of  $\Delta^{19}$  was *E*-form [11,12]. Therefore, **1** was determined as a new variotin derivative with a non-branched side chain and named variotin B [13].

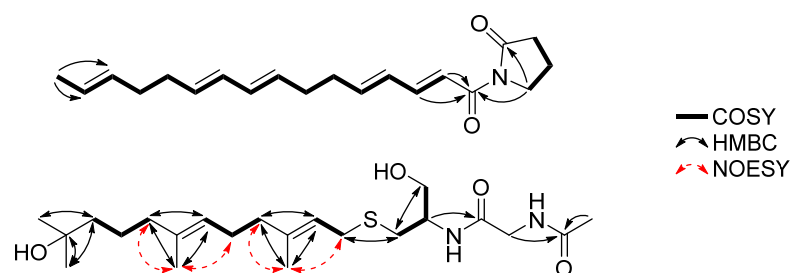


Figure 2. Key 2D NMR data of **1** and **2**.

Table 1.  $^1\text{H}$  and  $^{13}\text{C}$  NMR data of **1** and **2** in  $\text{CD}_3\text{OD}$  (600 MHz for  $^1\text{H}$  and 150 MHz for  $^{13}\text{C}$ ).

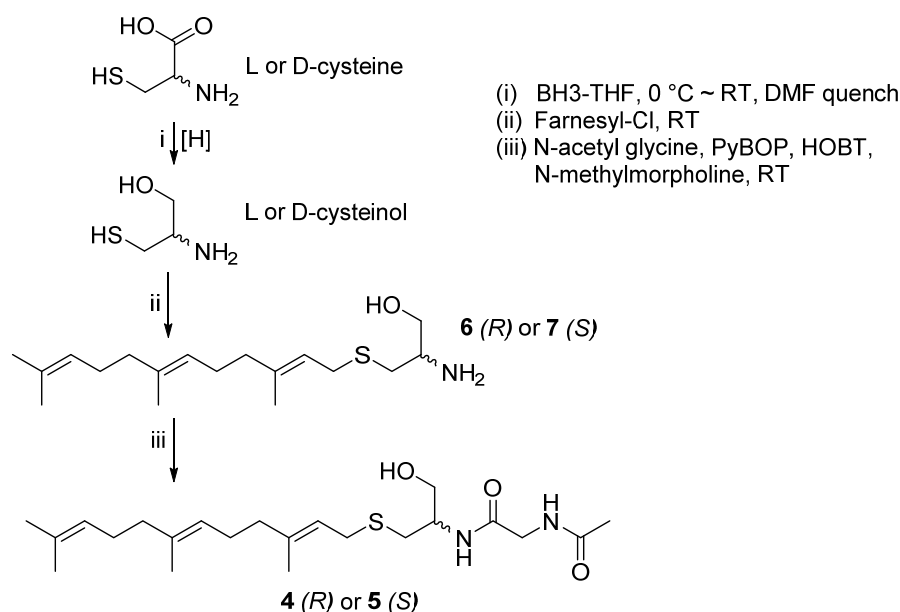
Compound	1		2	
Position	$\delta_{\text{H}}$ , mult ( $J$ in Hz)	$\delta_{\text{C}}$	$\delta_{\text{H}}$ , mult ( $J$ in Hz)	$\delta_{\text{C}}$
1		177.8	2.01, s	22.5
2	2.61, t (8.1)	34.6		173.9
3	2.04, m	18.1		
4	3.82, m	47.0	3.86, m	43.6
5				171.5
6		168.2		
7	7.25, d (15.1)	121.7	4.03, m	52.3
8	7.37, dd (15.1, 10.8)	146.9	2.55–2.70	32.9
9	6.32, dd (15.1, 10.8)	130.7		
10	6.23, m	146.0	3.16–3.22	30.3
11	2.29, q (6.6)	34.0	5.23, td (7.8, 1.0)	121.8
12	2.21, m	32.8		140.1
13	5.56, td (13.6, 6.6)	131.6	2.06, m	40.7
14	6.01, m	132.6	2.13, m	27.4
15	6.01, m	131.8	5.13, td (6.8, 1.0)	125.2
16	5.56, td (13.6, 6.6)	133.1		136.3
17	2.10, dd (14.1, 6.8)	33.6	1.98, t (7.2)	41.3
18	2.04, m	33.8	1.46, m	23.7
19	5.44, m	131.9	1.40, m	44.3
20	5.44, m	126.1		71.4
21	1.62, d (4.5)	18.1	1.17, s	29.2
22			1.17, s	29.2
23			1.61, s	16.0
24			1.68, s	16.2
25			3.62, m	63.6

Compound **2** was isolated as a colorless solid and its molecular formula was determined as  $\text{C}_{22}\text{H}_{40}\text{N}_2\text{O}_4\text{S}$ , with four indices of hydrogen deficiency based on its HRESIMS peak at  $m/z$  451.2607,  $([\text{M}+\text{Na}]^+)$ , calculated for  $\text{C}_{22}\text{H}_{40}\text{N}_2\text{O}_4\text{SNa}$ , 451.2606). The  $^1\text{H}$  NMR spectrum of **2** showed signals attributed to five methyl groups at  $\delta_{\text{H}}$  1.17 (s, 6H,  $\text{H}_3$ -21 and  $\text{H}_3$ -22), 1.61 (s,  $\text{H}_3$ -23), 1.68 (s,  $\text{H}_3$ -24), and 2.01 (s,  $\text{H}_3$ -1); seven methylene groups at  $\delta_{\text{H}}$  1.40–3.22; an oxygenated methylene group at  $\delta_{\text{H}}$  3.60 and 3.64 ( $\text{H}$ -25<sub>a,b</sub>); an amide methylene at  $\delta_{\text{H}}$  3.86 (m,  $\text{H}_2$ -4); an amide methine at  $\delta_{\text{H}}$  4.03 (m,  $\text{H}$ -7); and two olefinic protons at  $\delta_{\text{H}}$  5.13 and 5.23 (m,  $\text{H}$ -11 and  $\text{H}$ -15). The  $^{13}\text{C}$  NMR spectrum in combination with HSQC data demonstrated signals of 22 resonances belonging to five methyls at  $\delta_{\text{C}}$  16.0 (C-23), 16.2 (C-24), 22.5 (C-1), and 29.2 (2C, C-21 and C-22); seven methylenes at  $\delta_{\text{C}}$  23.7–44.3; an oxygenated methylene at  $\delta_{\text{C}}$  63.6; an amide methylene at  $\delta_{\text{C}}$  43.6; an amide methine at  $\delta_{\text{C}}$  52.3; a tertiary alcohol at  $\delta_{\text{C}}$  71.4; four olefinic carbons at  $\delta_{\text{C}}$  121.8–140.1; and

two carbonyl carbons at  $\delta_C$  171.5 and 173.9. Two carbonyl and four  $sp^2$  carbons accounting for all 4 degrees of unsaturation indicated **2** is an acyclic compound.

The structure of a cysteinol unit was determined by sequential  $^1H$ - $^1H$  COSY correlations of  $H_{8,a,b}/H_7/H_{25,a,b}$ . A partial structure of *N*-acetylglycine, which was connected to the cysteinol moiety via a peptide bond, was determined by the HMBC correlations of  $H_7/C-5$ ,  $H_{2-4}/C-2$ , and  $H_3-1/C-2$ . The remaining 15 carbons were assigned as a 10-hydroxy-11-hydroxyfarnesyl moiety based on a detailed analysis of  $^1H$ - $^1H$  COSY and HMBC data (Figure 2), and the connection of this moiety with the cysteinol residue via a thioether bond was determined by the HMBC correlations of  $H_{8,a,b}/C-10$  and  $H_{10,a,b}/C-8$ . The geometry of  $\Delta^{11}$  was deduced as *E*-form by the strong NOESY correlations from  $H_3-24$  to  $H_{10,a,b}$  and  $H_{13,a,b}$ ; and no-observed NOESY correlation from  $H_3-24$  to  $H_{11}$ . Similarly,  $\Delta^{15}$  was also determined as *E*-form (Figure 2). Consequently, the gross structure of **2** was determined as shown in Figure 1.

To determine the absolute configuration of **2**, we synthesized its analogs (**4** and **5**, a pair of enantiomers synthesized from *L*- and *D*-cysteine and farnesyl chloride, Scheme 1) from commercially available substances. By comparing the optical rotation sign of **2** [ $\alpha_D^{20}$  − 100 (*c* 0.3, MeOH)] with that of **4** [ $\alpha_D^{20}$  − 110 (*c* 0.3, MeOH)] and **5** [ $\alpha_D^{20}$  + 120 (*c* 0.3, MeOH)], the absolute configuration of **2** was determined to be the same as that of **4** (7*R*). Thus, **2** was determined as a new derivative of sulfur-containing natural products, coniosulfides A-D [14], and named coniosulfide E.



**Scheme 1.** Synthesis of **4** and **5**.

A co-isolated known compound was identified as unguisin A (**3**) by comparing its spectroscopic data with the corresponding literature values [6].

Since some fungal peptides were reported to show anti-inflammatory activity [4], **1** and **2** were evaluated for their anti-inflammatory activity. Subsequently, **1** showed moderate anti-inflammatory activity with an  $\text{IC}_{50}$  value of 20.0  $\mu\text{M}$ . Even though a literature review revealed many synthetic analogs of **2** demonstrated inhibitory effects on human isoprenylcysteine carboxyl methyltransferase (hIcmt) [15] or the inflammation process [16], unfortunately, **2** showed no anti-inflammatory activity at a concentration of 30.0  $\mu\text{M}$ . Due to the limited amount of **2**, we were unable to check its effect on hIcmt. Therefore, further studies are needed to find the bioactivities of **2**.

To further investigate the anti-inflammatory activity of **1**, we examined the inhibitory effect of **1** on lipopolysaccharide (LPS)-induced production of inflammatory mediators, including NO, IL-6, and iNOS, in RAW 264.7 cells. The treatment of RAW 264.7 cells

with LPS led to the accumulation of nitrite and IL-6, and **1** dose-proportionally inhibited LPS-induced production of nitrite and IL-6 in LPS-stimulated RAW 264.7 cells (Figure 3A,B). To further examine whether the effect of **1** were due to its effects on the mRNA expression of cognate genes, we investigated the effect of **1** on the mRNA expression of inducible nitric oxide synthase (iNOS) and IL-6 by quantitative polymerase chain reaction (qPCR). The mRNA levels of iNOS and IL-6 were induced by LPS treatment, and this induction was suppressed by **1** in a concentration-dependent manner (Figure 3C,D). Considering the above-mentioned data, it is noticeable that **1** showed anti-inflammatory activity by suppressing the production of NO and the expression of iNOS and IL-6 with no cytotoxicity at the treated concentrations. The results revealed that fungal natural products could be an important source of leads for the development of new anti-inflammatory drugs with minimal side effects.

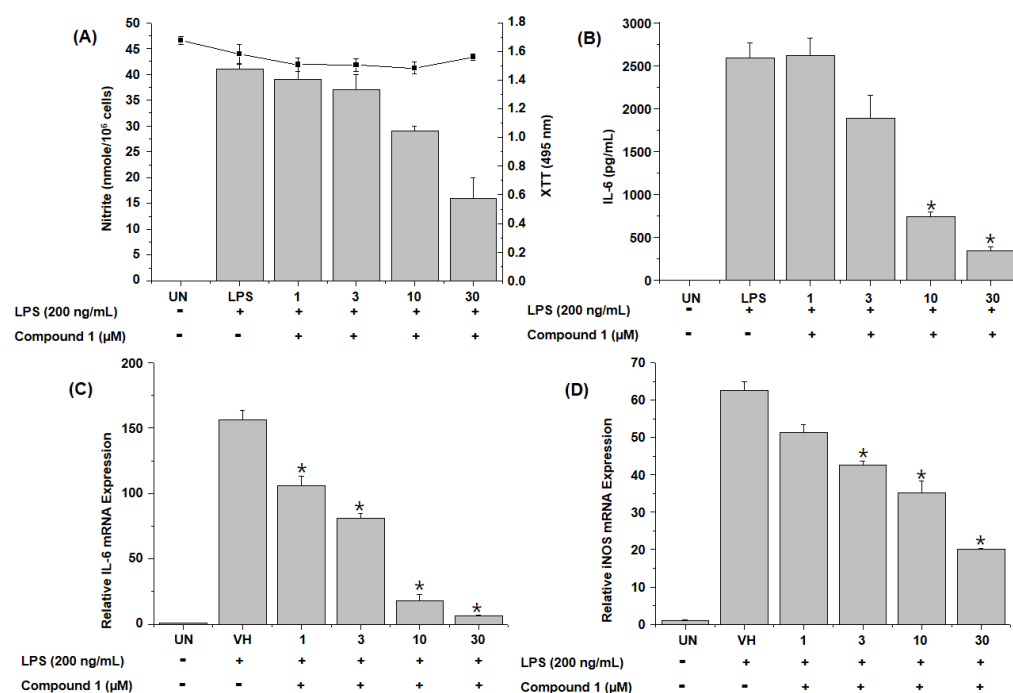


**Figure 3.** Inhibitory effects of **1** on LPS-induced nitrite production and IL-6 secretion in RAW 264.7 cells. RAW 264.7 cells were pretreated with **1** at the depicted concentrations (1–30  $\mu$ M) for 1 h and stimulated with LPS (200 ng/mL) for 24 h. The levels of nitrite (A) and IL-6 (B) in culture supernatants were determined by Griess reaction and ELISA, respectively. The mRNA levels of IL-6 (C) and iNOS (D) were examined by qPCR. Data are represented as the mean  $\pm$  SD of quadruplicate determinations. An asterisk (\*) denotes that the response is significantly different from vehicle-treated group as determined by Dunnett's multiple comparison test at  $p < 0.05$ . The results shown are representatives of more than two independent experiments (UN: Untreated; VH: Vehicle (0.1% DMSO)).

### 3. Materials and Methods

#### 3.1. General Experimental Procedures

HRESIMS data were obtained on a Waters Synapt G2 Q-TOF mass spectrometer (Waters Corporation, Milford, MA, USA). Optical rotations were measured on a Rudolph Research Analytical Autopol III polarimeter (Rudolph Research Analytical, Hackettstown, NJ, USA). 1D and 2D NMR spectra were acquired using a Bruker 600 MHz spectrometer (Bruker BioSpin GmbH, Rheinstetten, Germany). IR spectra were measured on a JASCO FT/IR-4100 spectrophotometer (JASCO Corporation, Tokyo, Japan). UV-visible spectra were measured by a Shimadzu UV-1650PC spectrophotometer. HPLC was carried out with a PrimeLine Binary pump (Analytical Scientific Instruments, Inc., El Sobrante, CA, USA) and a RI-101 detector (Shoko Scientific Co. Ltd., Yokohama, Japan). Semi-preparative HPLC was conducted using an ODS column (YMC-Pack-ODS-A, 250  $\times$  10 mm i.d, 5  $\mu$ M).

Analytical HPLC was performed with an ODS column (YMC-Pack-ODS-A, 250 × 4.6 mm i.d, 5 µm). All the used reagents were purchased from Sigma-Aldrich (Merck KGaA, Darmstadt, Germany).

### 3.2. Fungal Material, Fermentation, and Isolation of Secondary Metabolites

#### Fungal Material, Fermentation, and Isolation of 1–3 from *Aspergillus unguis* IV17-109

*A. unguis* IV17-109 (GenBank accession number OL700797) was isolated from a deep-sea shrimp sample as previously described [10]. The EtOAc extract was fractionated into 10 fractions (F1–F10), as described earlier [10]. The F7 fraction was purified by a semi-preparative reversed-phase HPLC (YMC-Pack-ODS-A, 250 × 10 mm i.d, 5 µm, flow rate 2.0 mL/min, 60% MeOH/H<sub>2</sub>O, RI detector) to obtain 3 (2.0 mg,  $t_R$  = 32 min). The F8 fraction was subjected to a semi-preparative reversed-phase HPLC (YMC-Pack-ODS-A, 250 × 10 mm i.d, 5 µm, flow rate 2.0 mL/min, RI detector) using an isocratic elution with 70% MeOH/H<sub>2</sub>O to yield a subfraction F8-1, and the subfraction was further purified by a semi-preparative HPLC (YMC-Pack-ODS-A, 250 × 10 mm i.d, 5 µm, flow rate 2.0 mL/min, RI detector) using an isocratic elution with 50% MeCN/H<sub>2</sub>O to obtain 2 (1.0 mg,  $t_R$  = 15 min). Finally, the F9 fraction was purified by a semi-preparative reversed-phase HPLC (YMC-Pack-ODS-A, 250 × 10 mm i.d, 5 µm, flow rate 2.0 mL/min, RI detector) using an isocratic elution with 83% MeOH/H<sub>2</sub>O to yield 1 (3.0 mg,  $t_R$  = 42 min).

Variotin B (1): pale-yellow needles; IR  $\nu_{\max}$  3286, 2918, 1724, 1671, 1352, 1261, 989 cm<sup>−1</sup>; UV(MeOH)  $\lambda_{\max}$  (log  $\epsilon$ ) 283 (2.51), 229 (2.60) nm; HRESIMS  $m/z$  336.1938 [M+Na]<sup>+</sup> (calcd for C<sub>20</sub>H<sub>27</sub>NO<sub>2</sub>Na, 336.1939), <sup>1</sup>H NMR (CD<sub>3</sub>OD, 600 MHz) and <sup>13</sup>C NMR (CD<sub>3</sub>OD, 150 MHz) see Table 1.

Coniosulfide E (2): colorless solid,  $[\alpha]_D^{20}$  − 100 (c 0.3, MeOH); IR  $\nu_{\max}$  3303, 2929, 1653, 1547, 1374, 1038 cm<sup>−1</sup>, HRESIMS  $m/z$  451.2607 [M+Na]<sup>+</sup> (calcd for C<sub>22</sub>H<sub>40</sub>N<sub>2</sub>O<sub>4</sub>SNa, 451.2606), <sup>1</sup>H NMR (CD<sub>3</sub>OD, 600 MHz) and <sup>13</sup>C NMR (CD<sub>3</sub>OD, 150 MHz) see Table 1.

### 3.3. Synthesis of 4 and 5

Compounds 4 and 5 were synthesized according to the reported procedures with minor modifications [17]. Borane-tetrahydrofuran (Borane-THF, 4 mL, 4 mmol) was added dropwise to L- or D-cysteine (0.121 g, 1 mmol) in dry THF (5 mL) at 0°C under a nitrogen atmosphere, and stirred at ambient temperature for 7 h. The reaction mixture was quenched with dry dimethylformamide (DMF, 1 mL) and stirred for 1 h. Farnesyl chloride (0.5 mmol) was added to the reaction mixture and stirred at room temperature for 3 h. The volatiles were removed in vacuo. The residue was re-dissolved in EtOAc (20 mL) and washed with H<sub>2</sub>O (20 mL) to remove the residue of cysteine. The EtOAc layer was evaporated under reduced pressure and the residue was purified by a semi-preparative HPLC using CH<sub>3</sub>OH/H<sub>2</sub>O (87:13) as an eluent to yield farnesyl-L-cysteinol (6) or farnesyl-D-cysteinol (7) (Figures S16 and S17).

To a dry DMF solution (500 µL) of 6 or 7 (5.0 mg) and N-acetylglycine (2.0 mg), benzotriazol-1-yloxytripyrrolidinophosphonium hexafluorophosphate (PyBOP, 12.0 mg), hydroxybenzotriazole (HOBT, 3.0 mg), and N-methylmorpholine (300 µL) were added [18]. The reaction mixture was stirred for 3 h at room temperature. Afterwards, 10 mL of water were added and the mixture was extracted twice with EtOAc (15 mL × 2). The EtOAc layer was dried, and the residue was purified by a semi-preparative HPLC (YMC-ODS column, 10 × 250 mm; MeCN-H<sub>2</sub>O, 65:35) to give compounds 4 or 5 with an overall yield of 11%.

1-farnesyl-2-(N-acetylglycine)-L-cysteinol (4): white amorphous solid,  $[\alpha]_D^{20}$  − 110 (c 0.3, MeOH), <sup>1</sup>H NMR (600 MHz, MeOD)  $\delta_H$  5.23 (t,  $J$  = 7.8 Hz, 1H), 5.14–5.07 (m, 2H), 4.05–4.00 (m, 1H), 3.90–3.82 (m, 2H), 3.64 (dd,  $J$  = 11.2, 5.2 Hz, 1H), 3.60 (dd,  $J$  = 11.1, 4.9 Hz, 1H), 3.22 (dd,  $J$  = 13.1, 8.0 Hz, 1H), 3.16 (dd,  $J$  = 13.1, 7.6 Hz, 1H), 2.70 (dd,  $J$  = 13.7, 6.5 Hz, 1H), 2.55 (dd,  $J$  = 13.7, 7.4 Hz, 1H), 2.11 (dt,  $J$  = 11.4, 5.8 Hz, 2H), 2.06 (dt,  $J$  = 14.2, 7.2 Hz, 4H), 2.01 (d,  $J$  = 1.0 Hz, 3H), 1.97 (t,  $J$  = 7.6 Hz, 2H), 1.68 (d,  $J$  = 7.2 Hz, 6H), 1.60 (s, 6H); <sup>13</sup>C NMR (150 MHz, MeOD)  $\delta_C$  173.8, 171.4, 140.1, 136.2, 132.1, 125.4, 125.2, 121.8, 63.6, 52.3,



43.6, 40.8, 40.7, 32.9, 30.4, 27.8, 27.5, 25.9, 22.5, 17.8, 16.2, 16.1; ESIMS  $m/z$  433.2  $[M + Na]^+$  (Figures S18–S22).

1-farnesyl-2-(*N*-acetyl glycine)-*D*-cysteinol (**5**): white amorphous solid,  $[\alpha]_D^{20} + 120$  (c 0.3, MeOH),  $^1H$  and  $^{13}C$  NMR, and ESIMS data of **5** were identical to those of **4** (Figures S23–S24).

### 3.4. Anti-Inflammatory Assay

Anti-inflammatory assay was conducted as described earlier [19]. Murine monocyte/macrophage RAW 264.7 (ATCC TIB-71) cell line was purchased from American Type Culture Collection (ATCC; Manassas, VA, USA).

## 4. Conclusions

In summary, based on NMR-guided isolation, two new (**1** and **2**) and one known (**3**) compounds were isolated from the culture broth of the deep-sea fungus *Aspergillus unguis* IV17-109. The planar structures of the new compounds were elucidated by a comprehensive analysis and comparison of their spectroscopic data with the values in the literature (HRESIMS, 1D, and 2D NMR). Compound **2** is a rare natural product with an unusual cysteinol moiety. The absolute configuration of **2** was determined by comparing its optical rotation sign with that of the synthesized analogs (**4** and **5**). Compounds **1** and **2** were preliminarily screened for their in vitro anti-inflammatory activity. Compound **1** showed moderate activity with an  $IC_{50}$  value of 20.0  $\mu M$ . To the best of our knowledge, this is the first report on linear nitrogenous secondary metabolites isolated from *Aspergillus unguis*. This research expanded the biological and chemical diversities of fungal natural products.

**Supplementary Materials:** The following are available online at <https://www.mdpi.com/article/10.3390/md20030217/s1>, Figures S1–S15, HRESIMS data,  $^1H$ ,  $^{13}C$ ,  $^1H$ - $^1H$  COSY, HSQC, HMBC, NOESY NMR experimental spectra of compounds **1** and **2**. Figures S16–S24, ESIMS,  $^1H$  NMR,  $^{13}C$  NMR experimental spectra of **4**–**7**.

**Author Contributions:** Conceptualization, H.J.S.; investigation, C.V.A. and Y.D.Y.; resources, H.-S.L. and C.-S.H.; writing—original draft preparation, C.V.A.; writing—review and editing, H.J.S.; visualization, J.S.K.; project administration, H.J.S.; funding acquisition, H.J.S. All authors have read and agreed to the published version of the manuscript.

**Funding:** This research was supported in part by the Korea Institute of Ocean Science and Technology (Grant PE99952) and the Ministry of Oceans and Fisheries, Republic of Korea (Grants PM62500 and no. 20170411).

**Institutional Review Board Statement:** Not applicable.

**Informed Consent Statement:** Not applicable.

**Data Availability Statement:** The data presented in the article are available in the Supplementary Materials.

**Acknowledgments:** The authors express gratitude to Jung Hoon Choi, Korea Basic Science Institute, Ochang, Korea, for providing mass data.

**Conflicts of Interest:** The authors declare no conflict of interest.

## References

1. Skropeta, D.; Wei, L. Recent advances in deep-sea natural products. *Nat. Prod. Rep.* **2014**, *31*, 999–1025. [CrossRef] [PubMed]
2. Andrianasolo, E.; Lutz, R.; Falkowski, P. Chapter 3—Deep-Sea Hydrothermal Vents as a New Source of Drug Discovery. *Stud. Nat. Prod. Chem.* **2012**, *36*, 43–66.
3. Pan, C.; Shi, Y.; Chen, X.; Chen, C.-T.A.; Tao, X.; Wu, B. New compounds from a hydrothermal vent crab-associated fungus *Aspergillus versicolor* XZ-4. *Org. Biomol. Chem.* **2017**, *15*, 1155–1163. [CrossRef] [PubMed]
4. Youssef, F.S.; Ashour, M.L.; Singab, A.N.B.; Wink, M. A Comprehensive Review of Bioactive Peptides from Marine Fungi and Their Biological Significance. *Mar. Drugs* **2019**, *17*, 559. [CrossRef] [PubMed]

5. Henke, M.T.; Soukup, A.A.; Goering, A.W.; McClure, R.A.; Thomson, R.J.; Keller, N.P.; Kelleher, N.L. New Aspercryptins, Lipopeptide Natural Products, Revealed by HDAC Inhibition in *Aspergillus nidulans*. *ACS Chem. Biol.* **2016**, *11*, 2117–2123. [CrossRef] [PubMed]
6. Malmström, J. Unguisins A and B: New Cyclic Peptides from the Marine-Derived Fungus *Emericella unguis*. *J. Nat. Prod.* **1999**, *62*, 787–789. [CrossRef] [PubMed]
7. Li, W.; Jiao, F.-W.; Wang, J.-Q.; Shi, J.; Wang, T.-T.; Khan, S.; Jiao, R.-H.; Tan, R.-X.; Ge, H.-M. Unguisin G, a new kynurenine-containing cyclic heptapeptide from the sponge-associated fungus *Aspergillus candidus* NF2412. *Tetrahedron Lett.* **2020**, *61*, 152322. [CrossRef]
8. Pahwa, R.; Goyal, A.; Jialal, I. *Chronic Inflammation*; StatPearls Publishing: Treasure Island, FL, USA, 2021. Available online: <https://www.ncbi.nlm.nih.gov/books/NBK493173/> (accessed on 25 February 2022).
9. Lee, H.-S.; Kang, J.S.; Choi, B.-K.; Lee, H.-S.; Lee, Y.-J.; Lee, J.; Shin, H.J. Phenazine Derivatives with Anti-Inflammatory Activity from the Deep-Sea Sediment-Derived Yeast-Like Fungus *Cystobasidium laryngis* IV17-028. *Mar. Drugs* **2019**, *17*, 482. [CrossRef] [PubMed]
10. Anh, C.V.; Kwon, J.-H.; Kang, J.S.; Lee, H.-S.; Heo, C.-S.; Shin, H.J. Antibacterial and Cytotoxic Phenolic Polyketides from Two Marine-Derived Fungal Strains of *Aspergillus unguis*. *Pharmaceuticals* **2022**, *15*, 74. [CrossRef] [PubMed]
11. Yonehara, H.; Takeuchi, S.; Umezawa, H.; Sumiki, Y. Variotin, a new antifungal antibiotic, produced by *Paecilomyces varioti* Bainier var. *antibioticus*. *J. Antibiot.* **1959**, *12*, 109–110.
12. Podkorytov, I.S.; Lubnin, A.V. <sup>13</sup>C NMR spectra of the models for the end-group analysis of polybutadiene. *Magn. Reson. Chem.* **1991**, *29*, 561–565. [CrossRef]
13. Ishii, T.; Nonaka, K.; Sugawara, A.; Iwatsuki, M.; Masuma, R.; Hirose, T.; Sunazuka, T.; Ōmura, S.; Shiomi, K. Cinatrins D and E, and virgaricin B, three novel compounds produced by a fungus, *Virgaria boninensis* FKI-4958. *J. Antibiot.* **2015**, *68*, 633–637. [CrossRef] [PubMed]
14. Vertesy, L.; Ehrlich, K.; Segeth, P.; Toti, L. Coniosulfides and Their Derivatives, Processes for Preparing Them, and Their Use as Pharmaceuticals. U.S. Patent US 2005/0209308A1, 22 September 2005.
15. Majmudar, J.D.; Morrison-Logue, A.; Song, J.; Hrycyna, C.A.; Gibbs, R.A. Identification of a novel nanomolar inhibitor of hIcmt via a carboxylate replacement approach. *Med. Chem. Comm.* **2012**, *3*, 1125–1137. [CrossRef]
16. Voronkov, M.; Perez, E.; Healy, J.; Fernandez, J. Preparation of Amino Acids for Treating or Preventing Inflammation, Acne, and Bacterial Conditions. International Patent WO 2018/132759 A1, 19 July 2018.
17. Rodriguez, D.; Ramesh, C.; Henson, L.H.; Wilmeth, L.; Bryant, B.K.; Kadavakollu, S.; Hirsch, R.; Montoya, J.; Howell, P.R.; George, J.M.; et al. Synthesis and characterization of tritylthioethanamine derivatives with potent KSP inhibitory activity. *Bioorg. Med. Chem.* **2011**, *19*, 5446–5453. [CrossRef] [PubMed]
18. Hwang, J.-Y.; Park, S.C.; Byun, W.S.; Oh, D.-C.; Lee, S.K.; Oh, K.-B.; Shin, J. Bioactive Bianthraquinones and Meroterpenoids from a Marine-Derived *Stemphylium* sp. Fungus. *Mar. Drugs* **2020**, *18*, 436. [CrossRef] [PubMed]
19. Shin, H.J.; Heo, C.-S.; Anh, C.V.; Yoon, Y.D.; Kang, J.S. Streptoglycerides E–H, Unsaturated Polyketides from the Marine-Derived Bacterium *Streptomyces specialis* and Their Anti-Inflammatory Activity. *Mar. Drugs* **2022**, *20*, 44. [CrossRef]